Original Article

Feasibility and reproducibility of cardiovascular magnetic resonance-feature tracking for quantitative right atrial function in dilated cardiomyopathy patients

Yiyuan Gao[1,2,3#], Jingjing Shi[1,2#], Yujing Shi[3,4], Lingnan Guo[1,2], Shanshan Zhou[3,5], Fan Zhang[1,2], Yifan Guo[1,2], Chen Gao[1,2], Ning Kong[1,2], Ping Xiang[1,2], Mingwu Lou[3], Maosheng Xu[1,2]

[1]Department of Radiology, The First Affiliated Hospital of Zhejiang Chinese Medical University (Zhejiang Provincial Hospital of Chinese Medicine), Hangzhou, China; [2]The First School of Clinical Medicine of Zhejiang Chinese Medical University, Hangzhou, China; [3]Shenzhen Clinical Medical College, Guangzhou University of Chinese Medicine, Shenzhen, China; [4]Department of Medical Ultrasound, Guangzhou First People's Hospital, Guangzhou, China; [5]Medical Imaging Research Institute of Longgang, The Third People's Hospital of Longgang District, Shenzhen, China

Contributions: (I) Conception and design: M Xu, Y Gao, J Shi; (II) Administrative support: M Xu, P Xiang; (III) Provision of study materials or patients: M Xu, M Lou; (IV) Collection and assembly of data: Y Gao, J Shi, Y Shi, L Guo, S Zhou; (V) Data analysis and interpretation: Y Gao, F Zhang, Y Guo, C Gao, N Kong; (VI) Manuscript writing: All authors; (VII) Final approval of manuscript: All authors.

[#]These authors contributed equally to this work.

Correspondence to: Maosheng Xu, MD. Department of Radiology, The First Affiliated Hospital of Zhejiang Chinese Medical University (Zhejiang Provincial Hospital of Chinese Medicine), 54 Youdian Road, Shangcheng District, Hangzhou 310018, China; The First School of Clinical Medicine of Zhejiang Chinese Medical University, Hangzhou, China. Email: xums166@zcmu.edu.cn.

Background: The importance of right heart assessment in dilated cardiomyopathy (DCM) is increasingly recognized. The development of cardiovascular magnetic resonance-feature tracking (CMR-FT) has provided a novel approach to quantify myocardial deformation and evaluate cardiac function. In this study, we aimed to evaluate the feasibility and reproducibility of CMR-FT for the quantitative derivation of right atrial (RA) strain and strain rate (SR) in patients with DCM.

Methods: A total of 68 DCM patients (84% male; aged 50.6±13.2 years) and 58 healthy controls (81% male; aged 48.4±11.2 years) were retrospectively enrolled from September 2018 to August 2022 at the First Affiliated Hospital of Zhejiang Chinese Medical University and Shenzhen Clinical Medical College of Guangzhou University of Chinese Medicine. RA reservoir, conduit, and booster strain (εs, εe, and εa) and peak positive, peak early negative, and peak late negative SR (SRs, SRe, and SRa) were measured using CMR-FT and compared between 2 groups using Student's *t*-test. Intra- and inter-observer reproducibility was evaluated using intraclass correlation coefficients (ICC) and Bland-Altman plots.

Results: Compared to healthy controls, DCM patients showed significantly lower RA strain (εs: 19.7%±9.0% *vs.* 44.4%±9.7%; εe: 7.9%±5.3% *vs.* 25.8%±8.6%; εa: 11.8%±6.2% *vs.* 18.6%±5.1%, all P<0.001) and SR (SRs: 1.17±0.48 *vs.* 1.92±0.62 s^{-1}; SRe: −0.85±0.56 *vs.* −1.94±0.63 s^{-1}; SRa: −1.39±0.71 *vs.* −2.01±0.65 s^{-1}, all P<0.001). There was no significant difference in RA maximum volume index between the 2 groups. Simple linear regression analysis demonstrated a significant correlation between N-terminal B-type natriuretic peptide (NT-proBNP), RA emptying fraction passive (RAEF passive), and RA εe [(NT-proBNP and εe): *r*=−0.48, P<0.001, 95% confidence interval (CI): −0.64 to −0.26; and (RAEF passive and εe): *r*=0.41, P=0.001, 95% CI: 0.22 to 0.56, respectively] in DCM patients. Intra- and inter-observer reproducibility was excellent (all ICCs >0.85) for RA deformation measurements.

Conclusions: CMR-FT is a promising, noninvasive approach for the quantitative assessment of RA phasic function in patients with DCM. DCM patients exhibit impaired RA reservoir, conduit, and booster pump

function prior to visible RA enlargement.

Keywords: Dilated cardiomyopathy (DCM); magnetic resonance imaging; atrial function; right; strain; strain rate (SR)

Submitted Aug 08, 2023. Accepted for publication Jan 17, 2024. Published online Apr 23, 2024.
doi: 10.21037/qims-23-1119
View this article at: https://dx.doi.org/10.21037/qims-23-1119

Introduction

Dilated cardiomyopathy (DCM) is a condition characterized by left or biventricular dilatation and contractile dysfunction, independent of abnormal preload conditions or severe coronary artery disease (1). As the main cause of heart failure (HF), DCM is the most common indication for heart transplant, with an estimated prevalence of 40 cases per 100,000 individuals (2,3). Previous studies have established the importance of assessing left ventricular (LV), left atrial (LA), and right ventricular (RV) enlargement and dysfunction in predicting the morbidity and mortality of DCM (4-8). However, limited attention has been given to exploring the potential presence and impact of right atrial (RA) dysfunction in patients with DCM.

The right atrium, despite its pivotal role in maintaining normal cardiac hemodynamics through reservoir, conduit, and booster pump function, is often overlooked in clinical assessment (9). Compared with the RA emptying fraction (RAEF), which is the most commonly used index for evaluating RA function, RA deformation parameters including strain and strain rate (SR) could provide a quantitative assessment of myocardial performance at all phases of the right atrium, and have been considered more sensitive indicators to detect the impairment of atrial phasic function (10-12). Increasing evidence has established that the assessment of RA function through myocardial deformation imaging possesses significant diagnostic and prognostic value in various cardiovascular diseases (13-15).

Speckle-tracking echocardiography (STE) is currently the preferred method for quantifying myocardial deformation (16). However, assessing RA function using STE may pose challenges due to the RA anatomical complexity, thin wall and appendage, and the presence of the superior vena cava. Conversely, cardiovascular magnetic resonance-feature tracking (CMR-FT), a novel technique based on routine balanced steady-state free precession (SSFP) cine sequences, offers higher spatial resolution, better reproducibility, and improved definition of endocardial borders, making it increasingly attractive for evaluating RA phasic functions (17). Moreover, a very recent study using a fast long-axis method found that RA strain was closely associated with poor outcomes in patients with DCM (18). Nonetheless, studies focused on RA deformation using CMR-FT in DCM patients are limited.

Therefore, the primary objective of the present study was to determine the feasibility and reproducibility of CMR-FT for quantifying RA function in patients with DCM, and investigate the potential differences in RA phasic function between DCM patients and healthy individuals. We present this article in accordance with the STROBE reporting checklist (available at https://qims.amegroups.com/article/view/10.21037/qims-23-1119/rc).

Methods

Study population

The study was conducted in accordance with the Declaration of Helsinki (as revised in 2013). The study was approved by the Ethics Committees of The First Affiliated Hospital of Zhejiang Chinese Medical University (2022-KLS-207-01) and Shenzhen Clinical Medical College of Guangzhou University of Chinese Medicine (2021ECPJ006), and the requirement for individual consent for this retrospective analysis was waived. The study enrolled a total of 68 consecutive patients with non-ischemic, idiopathic DCM who underwent CMR examinations at The First Affiliated Hospital of Zhejiang Chinese Medical University and Shenzhen Clinical Medical College of Guangzhou University of Chinese Medicine from September 2018 to August 2022. Thirty patients have been reported in a previous study, which was aimed to predict outcomes in DCM (19). DCM was defined as having an LV ejection fraction (EF) <50% and an indexed LV end-diastolic diameter >33 mm/m^2 for men or >32 mm/m^2 for women (20). The exclusion criteria were as follows: (I) ischemic heart diseases, characterized by a history of myocardial infarction,

greater than 50% luminal stenosis at coronary angiography, or infarct pattern of late gadolinium enhancement (LGE) on CMR; (II) hypertrophic, restrictive, or infiltrative cardiomyopathy; (III) severe valvular diseases; (IV) congenital heart diseases; (V) acute myocarditis; (VI) arrhythmogenic RV cardiomyopathy (Figure S1). All DCM patients completed fasting routine laboratory and biochemical tests [including fasting blood glucose, N-terminal B-type natriuretic peptide (NT-proBNP), etc.] within 3 days before or after CMR examination. As the control group, 58 age- and gender-matched healthy individuals without hypertension, diabetes, and overt cardiovascular diseases were enrolled at The First Affiliated Hospital of Zhejiang Chinese Medical University.

CMR protocol

CMR images were acquired with 3.0T CMR scanners (Magnetom Prisma, Siemens Healthineers, Erlangen, Germany, and Discovery MR750, General Electric Healthcare, Chicago, IL, USA) scanners with 16- or 32-channel phased-array surface coil. Cases underwent imaging in a supine position, and SSFP cine images were acquired covering the whole left ventricle, continuously from the base to the apex on short-axis views and long-axis views (2-, 3-, and 4-chamber) covering the whole heart by breath-holding and retrospective electrocardiographic (ECG) gating. Typical image parameters were as follows: repetition time (TR) =3.1 ms, echo time (TE) =1.5 ms, field of view (FOV) =350×350 mm, matrix size =176×150, slice thickness =8 mm, slice gaP =2 mm, and 30 phases per cardiac cycle (Magnetom Prisma); TR =3.2 ms, TE =1.4 ms, FOV =340×340, matrix size =224×160, slice thickness =8 mm, slice gaP =2 mm, and 25–30 phases per cardiac cycle (Discovery MR750). LGE images were acquired using the phase-sensitive inversion recovery sequence at 10–15 minutes following the injection of gadolinium at a dosage of 0.15 mmol/kg per bolus. The scan parameters were as follows: TR =2.8 ms, TE =1.4 ms, FOV =326×360 mm, matrix size =128×192, slice thickness =8 mm, slice gaP =2 mm, temporal resolution =42 ms, and 30 phases per cardiac cycle (Magnetom Prisma); TR =2.4 ms, TE =1.1 ms, FOV =320×320, matrix size =128×128, slice thickness =8 mm, slice gaP =2 mm, temporal resolution =48 ms, and 25–30 phases per cardiac cycle (Discovery MR750).

CMR image analysis

All CMR images were imported into commercially available software (cvi42® version 5.14.2; Circle Cardiovascular Imaging, Calgary, Canada), and were subsequently analyzed in a blinded fashion by an experienced researcher (Y. Gao with more than 5 years of experience in CMR analysis). Upon visual inspection, the frames exhibiting the minimal blood pool in the midst of the ventricular chamber were designated as representing end-systole, whereas those with the maximal blood pool were defined as end-diastole. LV and RV endocardial and epicardial contours were manually drawn using a point-and-click approach in end-systole and end-diastole, respectively. Biventricular end-diastolic volume (EDV), end-systolic volume (ESV), stroke volume (SV), and EF were measured on the short-axis cine images. LV mass (LVM) was obtained from the end-diastolic frames. Heart rate (HR) was measured during the CMR scan. Cardiac output (CO) was obtained by multiplying SV and HR. LA volumes were assessed in the 2- and 4-chamber views using the biplane area-length method (21).

RA endocardial contours were manually tracked in the 4-chamber view. RA maximal volume (RAVmax, at the ventricular end-systole), pre-atrial contractile volume (RAVpac, at the ventricular diastole before RA contraction), and minimal volume (RAVmin, at the late ventricular end-diastole after RA contraction) were automatically obtained according to the single area-length method (21). Total RA emptying fraction (RAEF total, corresponding to atrial reservoir function), passive RA emptying fraction (RAEF passive, corresponding to atrial conduit function), and active RA emptying fraction (RAEF booster, corresponding to atrial contractile booster pump function) were defined as fractional volume changes according to the following equations: RAEF total = (RAVmax – RAVmin) × 100/RAVmax; RAEF passive = (RAVmax × RAVpac) × 100/RAVmax; and RAEF booster = (RAVpac × RAVmin) × 100/RAVpac (20).

Biventricular and biatrial volumes were normalized to body surface area (BSA). BSA was calculated using the Mosteller formula: BSA (m^2) = [height (cm) × weight (kg)/3,600]$^{1/2}$.

CMR-FT analysis for RA

RA deformation parameters were analyzed using commercially available software (cvi42® version 5.14.2, Circle Cardiovascular Imaging) by a researcher (Y. Gao). The basic information of cases, such as age and sex, was concealed throughout the CMR-FT analysis. RA endocardial and epicardial borders were manually traced in

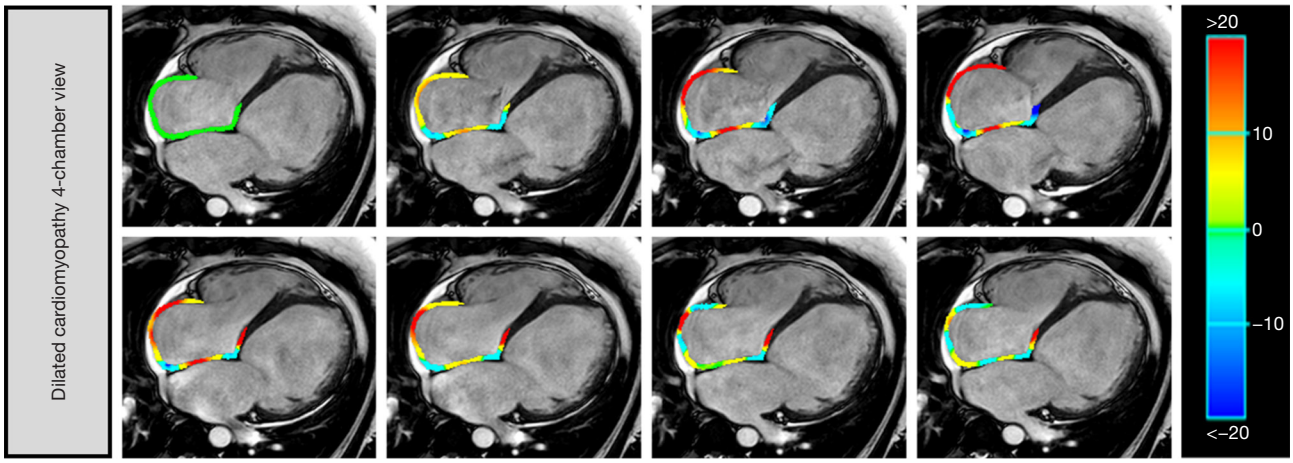

Figure 1 An example of RA cardiovascular magnetic resonance-feature tracking analysis in a patient with dilated cardiomyopathy in the 4-chamber view. RA, right atrial.

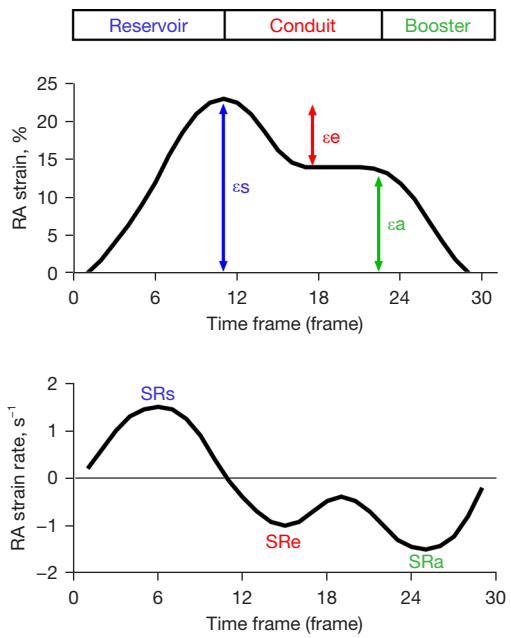

Figure 2 RA strain and strain rate curve. RA phasic function including reservoir, conduit, and booster pump function. RA εs and SRs correspond to reservoir function. RA εe and SRe correspond to conduit function. RA εa and SRa correspond to booster pump function. RA, right atrial; εs, reservoir strain; εe, conduit strain; εa, booster strain; SR, strain rate; SRs, peak positive SR; SRe, peak early negative SR; SRa, peak late negative SR.

the 4-chamber views using a point-and-click approach at the minimum RA volume after atrial contraction (11). The superior vena cava and RA appendage were excluded from the RA endocardial contours and the automated tracking algorithm was subsequently applied. Tracking performance was visually checked to ensure accurate tracking of the RA myocardium and the initial contours were manually adjusted when necessary (*Figure 1*). The longitudinal RA strain and SR values were obtained using feature tracking analyses in the 4-chamber views. We analyzed 3 aspects of RA strain and SR (22): reservoir strain and peak positive SR (εs and SRs, corresponding to atrial reservoir function during RV end-systole), conduit strain and peak early negative SR (εe and SRe, corresponding to atrial conduit function during RV early diastole), and booster strain and peak late negative SR (εa and SRa, corresponding to atrial booster pump function during RV late diastole) (*Figure 2*).

Reproducibility

The intra- and inter-observer reproducibility for RA deformation measurements was evaluated in 40 randomly selected DCM patients. Intra-observer reproducibility was assessed by the first author who re-analyzed the same 40 patients after 1 month. Inter-observer reproducibility was analyzed by 2 independent observers, blinded to measurements (Y. Gao and J. Shi with more than 5 years of experience).

Statistical analysis

All statistical analyses were conducted utilizing SPSS (version 26.0; IBM Corp., Armonk, NY, USA) and

GraphPad Prism (version 8.0.2; GraphPad Software, La Jolla, CA, USA). Continuous variables following normal distribution were depicted as mean ± standard deviation (SD), whereas those not normally distributed are represented as median (interquartile range). Categorical variables were presented as frequencies and percentages. Comparison of the continuous variables between the 2 groups was conducted using the Student's *t*-test for normally distributed data, the Mann-Whitney U test for non-normally distributed data, and the chi-square test for categorical variables. Simple linear regression analysis was applied to investigate the correlation between NT-pro BNP, RAEF, and RA deformation parameters. Correlations were deemed weak with a coefficient <0.3, moderate at 0.3–0.5, and strong when >0.5. Intra- and inter-observer reproducibility was analyzed using intraclass correlation coefficients (ICC) and Bland-Altman plots. Reproducibility was considered as excellent with an ICC exceeding 0.74, good within the 0.60–0.74 range, fair from 0.40 to 0.59, and poor below 0.40 (23). A 2-sided P value <0.05 was considered significant.

Results

Baseline characteristics

The baseline characteristics of the study population are shown in *Table 1*. There were no significant differences in gender, age, body height, BSA, and fasting blood glucose between the 2 groups (all P>0.05). Compared with healthy controls, DCM patients demonstrated significantly higher systolic blood pressure (SBP), diastolic blood pressure (DBP), and HR (all P<0.05). In the DCM group, 6 patients were New York Heart Association (NYHA) class I, 30 were NYHA class II, 23 were NYHA class III, and 9 were NYHA class IV.

Biventricular and LA conventional parameters

Biventricular and LA structure and function parameters are presented in *Table 2*. Compared with healthy controls, patients with DCM demonstrated significantly higher LVEDV index (LVEDVi), LVESV index (LVESVi), LV mass, RVEDV index (RVEDVi), RVESV index (RVESVi), LA maximal volume index (LAVmaxi), LA minimal volume index (LAVmini), and LA pre-atrial contractile volume index (LAVpaci) (all P<0.05). Moreover, LVSV index (LVSVi), LVEF, RVSV index (RVSVi), RV ejection fraction (RVEF), and RV cardiac output (RVCO) in DCM patients were significantly lower than those in healthy controls (all P<0.05). There was no significant difference in LV cardiac output (LVCO) between the 2 groups (P=0.63). The presence of LGE was observed in 33 of the total DCM patients.

RA volumetric and deformation parameters

There was no significant difference in the RAVmax index (RAVmaxi) between DCM patients and healthy controls (P=0.17). Compared with healthy controls, patients with DCM had significantly higher RAVmin index (RAVmini) and RAVpac index (RAVpaci), and lower RAEF total, RAEF passive, and RAEF booster. RA CMR-FT was successfully performed in all cases. The magnitudes of RA deformation parameters, including εs, εe, εa, SRs, SRe, and SRa, in DCM patients were all significantly lower than those in healthy controls (all P<0.05) (*Table 3*).

Correlation between NT-proBNP, RAEF, and RA deformation parameters in DCM patients

Simple linear regression analysis demonstrated weak-to-moderate correlation between RA εs, εe, and NT-proBNP [(εs and NT-proBNP): r=–0.27, P=0.03, 95% confidence interval (CI): –0.48 to –0.02; and (εe and NT-proBNP): r=–0.48, P<0.001, 95% CI: –0.64 to –0.26] (*Table 4*). Moreover, RA deformation parameters were moderately to strongly correlated with RAEFs for RA reservoir, conduit, and booster pump function in DCM patients [(εs and RAEF total): r=0.64, P<0.001, 95% CI: 0.50 to 0.75; (εe and RAEF passive): r=0.41, P=0.001, 95% CI: 0.22 to 0.56; and (εa and RAEF booster): r=0.50, P<0.001, 95% CI: 0.34 to 0.64] (*Table 4*, *Figure 3*).

Reproducibility

Intra- and inter-observer reproducibility for RA deformation measurements are shown in *Table 5* and *Figures 4,5*. These results demonstrated good-to-excellent reproducibility for RA strain and SR derived from CMR-FT with all ICCs >0.75 and narrow limits of agreement in Bland-Altman plots.

Discussion

To the best of our knowledge, this is the first study to

Table 1 Baseline characteristics of the study population

Characteristics	DCM (n=68)	Healthy controls (n=58)	P value
Age (years)	50.6±13.2	48.4±11.2	0.33
Male gender, n (%)	57 (84.0)	47 (81.0)	0.99
Body height (cm)	167.6±7.3	167.7±8.2	0.98
BMI (kg/m^2)	24.5±3.8	23.5±2.6	0.09
BSA (m^2)	1.79±0.19	1.75±0.17	0.30
SBP (mmHg)	125.3±15.2	114.8±11.4	<0.001
DBP (mmHg)	83.1±15.6	73.1±8.7	<0.001
Heart rate (bpm)	76.2±12.5	64.6±8.9	<0.001
NT-proBNP (pg/mL)	1,675.0 (519.8–4,832.5)	–	–
FBG (mmol/L)	5.44±2.11	5.26±0.52	0.52
Hypertension, n (%)	28 (41.2)	–	–
Diabetes, n (%)	12 (17.7)	–	–
NYHA class, n (%)			
I	6 (8.8)	–	–
II	30 (44.1)	–	–
III	23 (33.8)	–	–
IV	9 (13.2)	–	–
Medication, n (%)			
Beta-blocker	58 (85.3)	–	–
ACEI/ARB	56 (82.4)	–	–
Calcium blocker	9 (13.2)	–	–
Diuretics	56 (82.4)	–	–

Data were presented as percentages in parentheses, means ± standard deviations or median (interquartile range). P values were obtained from the Student's *t*-test or chi-squared test. DCM, dilated cardiomyopathy; BMI, body mass indexed; BSA, body surface area; SBP, systolic blood pressure; DBP, diastolic blood pressure; NT-proBNP, N-terminal pro-brain natriuretic peptide; FBG, fasting blood glucose; NYHA, New York Heart Association; ACEI/ARB, angiotensin-converting enzyme inhibitors/angiotensin II receptor blockers.

evaluate RA phasic function in DCM patients using CMR-FT. The main findings of the present study were the following: (I) CMR-FT is a promising tool for the quantitative assessment of RA myocardial deformation in DCM patients, with considerably high reproducibility; (II) RA reservoir, conduit, and booster pump dysfunction were observed in patients with DCM prior to visible RA enlargement, as evidenced by the decreased magnitudes of RA εs, εe, εa, SRs, SRe, and SRa, and the preserved RAVmaxi; (III) there was a significant correlation between NT-proBNP, RAEF, and CMR-FT-derived RA deformation parameters in DCM patients.

Feasibility and reproducibility of RA deformation measurements based on CMR-FT

In the present study, CMR-FT of RA myocardium was successfully performed in all DCM patients, highlighting its favorable feasibility for evaluating RA phasic function in this population. Although CMR-FT is being increasingly used to evaluate RA myocardial deformation, there remains limited quantitative data concerning the reproducibility of these measurements, particularly in patients with DCM. Our study addressed this gap and demonstrated that RA strain and SR measurements using CMR-FT exhibited good intra- and inter-observer reproducibility in DCM patients.

Table 2 Comparison of biventricular and left atrial conventional parameters between DCM patients and healthy controls

Variables	DCM (n=68)	Healthy controls (n=58)	P value
Left ventricle			
LVEDVi (mL/m^2)	150.0±50.2	61.2±9.3	<0.001
LVESVi (mL/m^2)	113.6±49.4	19.4±4.9	<0.001
LVSVi (mL/m^2)	35.6±8.4	41.8±7.0	<0.001
LVEF (%)	25.6±9.3	68.5±5.9	<0.001
LVCO (L/min)	5.02±1.55	4.90±1.20	0.63
LV mass (g)	173.4±56.4	113.9±23.8	<0.001
LGE, n (%)	33 (48.5)	–	–
Right ventricle			
RVEDVi (mL/m^2)	86.1±28.1	70.0±11.7	<0.001
RVESVi (mL/m^2)	55.8±25.2	28.3±7.5	<0.001
RVSVi (mL/m^2)	30.0±10.3	41.7±6.8	<0.001
RVEF (%)	36.8±12.6	60.0±6.2	<0.001
RVCO (L/min)	4.20±1.69	4.89±1.18	0.01
Left atrium			
LAVmaxi (mL/m^2)	54.1±28.2	33.1±8.5	<0.001
LAVmini (mL/m^2)	41.2±27.8	12.7±4.2	<0.001
LAVpaci (mL/m^2)	47.8±27.6	21.7±6.9	<0.001

Data were presented as percentages in parentheses or given as means ± standard deviations. P values were obtained from the Student's *t*-test. DCM, dilated cardiomyopathy; LVEDVi, LV end-diastolic volume index; LVESVi, LV end-systolic volume index; LVSVi, LV stroke volume index; LVEF, LV ejection fraction; LVCO, LV cardiac output; LV, left ventricular; LGE, late gadolinium enhancement; RVEDVi, RV end-diastolic volume index; RVESVi, RV end-systolic volume index; RVSVi, RV stroke volume index; RVEF, RV ejection fraction; RVCO, RV cardiac output; LAVmaxi, LA maximum volume index; LAVmini, LA minimum volume index; LAVpaci, left pre-atrial contraction volume index; RV, right ventricular; LA, left atrial.

This finding aligns with a previous study conducted in healthy participants (15). The excellent reproducibility observed in RA deformation measurements with CMR-FT may be attributed to the high spatial resolution and image quality provided by CMR. These factors enable the clear identification and reliable delineation of the thin RA myocardium, enhancing the accuracy of the tracking algorithm. Overall, our study underscores the reliability of CMR-FT for assessing RA function, supporting its clinical utility in the evaluation of DCM patients.

Comparison of RA parameters between DCM patients and healthy cases

In accordance with several previous studies based on STE or the fast long-axis method (18,24), we demonstrated that the RA reservoir, conduit, and booster pump function were all impaired in DCM patients, as evidenced by the decreased magnitudes of RA εs, εe, εa, SRs, SRe, and SRa. The mechanism of RA dysfunction in patients with DCM has not been fully elucidated. Secondary pulmonary hypertension due to elevated LV filling pressure causes RV dysfunction and remodeling, which ultimately results in a decline in RA function (25,26). Moreover, RA fibrosis and functional tricuspid regurgitation caused by RV dilatation in DCM may also be responsible for RA dysfunction (27,28). Regarding the presence or absence of RA enlargement in patients with DCM, results had been controversial. Specifically, Bogaert *et al.* (29) reported that DCM patients with RV dysfunction had greater indexed RA area compared with healthy volunteers, whereas Järvinen *et al.* (30) found that RA maximum volume was comparable between mildly

Table 3 Comparison of RA parameters between the DCM patients and healthy controls

Variables	DCM (n=68)	Healthy controls (n=58)	P value
RA volume index (mL/m^2)			
RAVmaxi	38.9±15.0	35.9±8.0	0.17
RAVmini	24.6±13.2	18.9±4.8	0.002
RAVpaci	33.1±13.8	28.7±6.8	0.03
RA function volumetric (%)			
RAEF total	39.5±12.4	47.4±6.3	<0.001
RAEF passive	15.6±7.8	19.9±7.0	0.002
RAEF booster	28.6±11.5	34.1±7.6	0.002
RA strain (%)			
εs	19.7±9.0	44.4±9.7	<0.001
εe	7.9±5.3	25.8±8.6	<0.001
εa	11.8±6.2	18.6±5.1	<0.001
RA strain rate (s^{-1})			
SRs	1.17±0.48	1.92±0.62	<0.001
SRe	−0.85±0.56	−1.94±0.63	<0.001
SRa	−1.39±0.71	−2.01±0.65	<0.001

Data were presented as means ± standard deviations. P values were obtained from the Student's *t*-test. RA, right atrial; DCM, dilated cardiomyopathy; RAVmaxi, RA maximum volume index; RAVmini, RA minimum volume index; RAVpaci, right pre-atrial contraction volume index; RAEF, RA emptying fraction; εs, reservoir strain; εe, conduit strain; εa, booster strain; SRs, peak positive SR; SRe, peak early negative SR; SRa, peak late negative SR; SR, strain rate.

Table 4 Association of NT-proBNP and RAEF with RA strain and SR in the DCM group (n=68)

Variables	NT-proBNP			RAEF total			RAEF passive			RAEF booster		
	r	95% CI	P value	r	95% CI	P value	r	95% CI	P value	r	95% CI	P value
RA εs	−0.27	(−0.48, −0.02)	0.03	0.64	(0.50, 0.75)	<0.001	0.36	(0.17, 0.52)	0.003	0.61	(0.46, 0.72)	<0.001
RA εe	−0.48	(−0.64, −0.26)	<0.001	0.52	(0.36, 0.65)	<0.001	0.41	(0.22, 0.56)	0.001	0.44	(0.26, 0.59)	<0.001
RA εa	0.00	(−0.25, 0.24)	0.99	0.48	(0.31, 0.62)	<0.001	0.17	(−0.03, 0.36)	0.16	0.50	(0.34, 0.64)	<0.001
RA SRs	−0.27	(−0.49, −0.03)	0.03	0.48	(0.31, 0.62)	<0.001	0.40	(0.22, 0.56)	0.001	0.36	(0.17, 0.53)	0.002
RA SRe	0.28	(0.03, 0.49)	0.02	−0.43	(−0.58, −0.25)	<0.001	−0.47	(−0.62, −0.30)	<0.001	−0.25	(−0.43, −0.05)	0.04
RA SRa	−0.10	(−0.34, −0.14)	0.40	−0.44	(−0.59, −0.26)	<0.001	−0.26	(−0.44, −0.07)	0.03	−0.39	(−0.55, −0.21)	0.001

P values were obtained from the simple linear regression analysis. NT-proBNP, N-terminal pro-brain natriuretic peptide; RAEF, RA emptying fraction; RA, right atrial; SR, strain rate; DCM, dilated cardiomyopathy; CI, confidence interval; εs, reservoir strain; εe, conduit strain; εa, booster strain; SRs, peak positive SR; SRe, peak early negative SR; SRa, peak late negative SR.

symptomatic DCM patients and healthy cases. In the present study, we observed no significant difference in RAVmaxi between DCM patients and healthy controls. The authors speculated that the differences in baseline characteristics and disease progression of patients may be responsible for these discrepancies among studies. Overall, our observations suggested that RA dysfunction may occur prior to RA enlargement in patients with DCM.

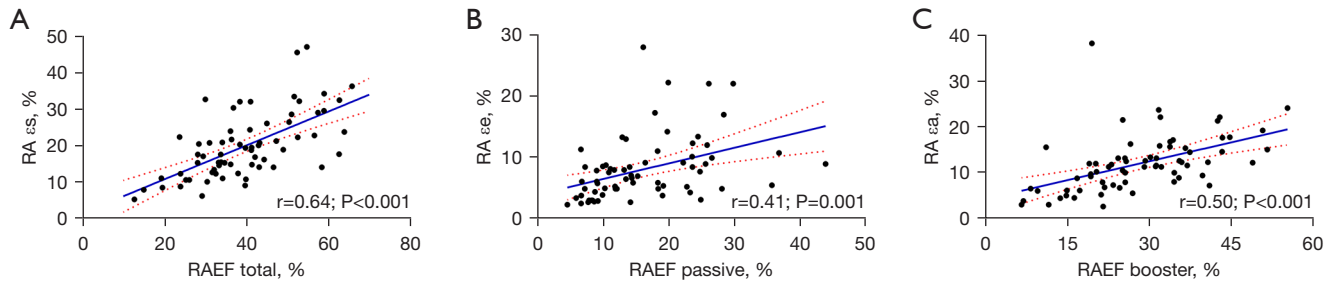

Figure 3 Correlation between RA strain and RAEF for RA reservoir (A), conduit (B) and booster (C) pump function in dilated cardiomyopathy patients. RA, right atrial; εs, reservoir strain; εe, conduit strain; εa, booster strain; RAEF, RA emptying fraction.

Table 5 Intra-observer and inter-observer reproducibility for RA deformation parameters in the DCM group (n=40)

Variables	Intra-observer		Inter-observer	
	Mean difference ± SD	ICC (95% CI)	Mean difference ± SD	ICC (95% CI)
εs (%)	0.69±3.75	0.916 (0.847–0.954)	0.13±3.62	0.911 (0.839–0.952)
εe (%)	0.71±2.41	0.912 (0.838–0.953)	0.01±2.43	0.901 (0.820–0.946)
εa (%)	–0.02±2.83	0.888 (0.798–0.939)	0.13±3.03	0.872 (0.771–0.930)
SRs (s^{-1})	0.02±0.30	0.829 (0.699–0.906)	–0.01±0.34	0.786 (0.631–0.881)
SRe (s^{-1})	0.04±0.29	0.848 (0.732–0.916)	0.02±0.37	0.781 (0.622–0.878)
SRa (s^{-1})	0.01±0.34	0.874 (0.774–0.931)	0.04±0.43	0.815 (0.678–0.898)

RA, right atrial; DCM, dilated cardiomyopathy; SD, standard deviation; ICC, intraclass correlation coefficient; CI, confidence interval; εs, reservoir strain; εe, conduit strain; εa, booster strain; SRs, peak positive; SRe, peak early negative SR; SRa, peak late negative SR; SR, strain rate.

Association of NT-proBNP and RAEF with RA deformation parameters in the DCM group

NT-proBNP is a neurohormone synthesized and released by the atrial cells, which is considered a useful and reliable biomarker in diagnosing and predicting HF (31). Additionally, it has been shown to be valuable in risk stratification for various cardiovascular diseases (32,33). In this study, we confirmed a significant correlation between RA εs, εe, SRs, SRe, and NT-proBNP, suggesting that RA deformation parameters may provide valuable insight into the progression or severity of DCM. Moreover, we observed significant correction between CMR-FT-derived RA deformation parameters and RAEFs for atrial reservoir, conduit, and booster pump function, which was consistent with previous studies (34,35).

Clinical utility

Contrary to the perception of being a passive chamber, the right atrium plays an essential role in modulating ventricular filling and maintaining normal cardiac hemodynamics: as a reservoir during RV systole, a conduit from the vena cava and coronary sinus to the RV during early diastole and a booster pump in late diastole (11). Previous studies have reported that RA function is tightly related to morbidity and mortality of multiple cardiovascular diseases, such as pulmonary hypertension, HF, and myocardial infarction (36-38). Furthermore, evidence indicates that over 20% of patients with DCM exhibit a higher risk of pulmonary hypertension, and the longer the duration of DCM, the higher the likelihood of developing pulmonary hypertension (39), indicating a potential presence of right heart dysfunction in DCM. Our study further supports this notion by demonstrating RA phasic dysfunction in DCM patients. Therefore, the quantitative evaluation of RA deformation parameters may contribute to the early diagnosis, risk stratification, and prognosis assessment in DCM patients. By providing insights into RA function, CMR-FT offers a promising noninvasive approach to assess the subtle changes in the right atrium, potentially aiding in the management and decision-making process for DCM patients.

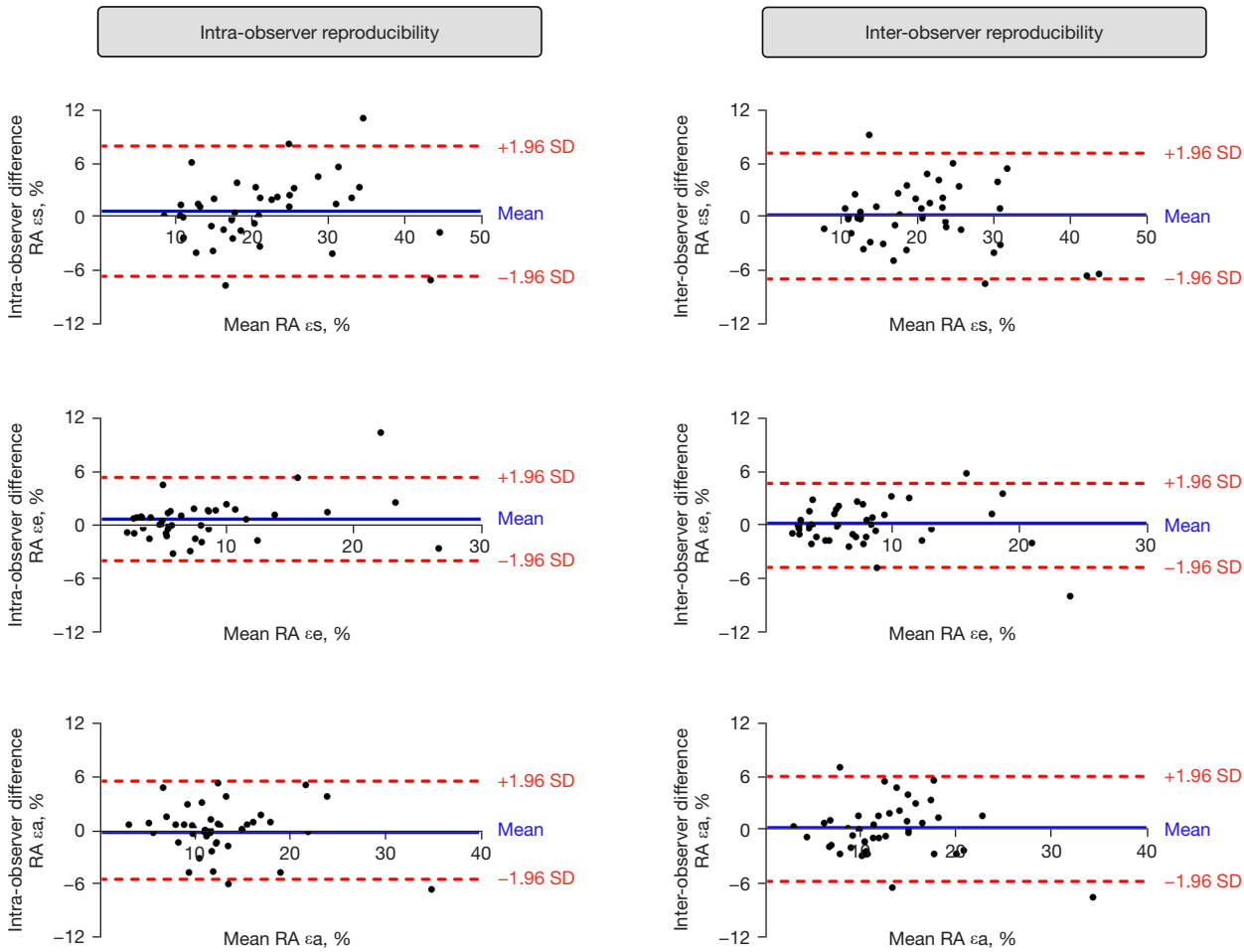

Figure 4 Bland-Altman plots for intra- and inter-observer reproducibility of RA εs, εe, and εa. SD, standard deviation; RA, right atrial; εs, reservoir strain; εe, conduit strain; εa, booster strain.

Moreover, regarding post-processing time, RAEF takes approximately 3 minutes, which is slightly longer than the RA strain measurement, typically around 1–2 minutes. The process differs as RAEF requires delineation of the RA contour at 3 different cardiac phases (LV end-systole, pre-atrial contraction, and LV end-diastole phase), whereas RA strain necessitates outlining only at the end of LV diastole. Both methods have be shown to be robust for measuring RA function, but RA strain may be more time-efficient due to its simpler procedure.

Limitations

There are several limitations in the present study. First, this was a retrospective study with a relatively small sample size, which may be subjected to selection bias. However, as a feasibility and reproducibility study, the sample size was sufficient to respond to its main objective. Second, the present study was conducted within an Eastern-only population. Given the potential racial differences in RA deformation parameters, our results should be carefully extrapolated to other ethnic groups. Third, we did not perform direct comparisons with STE, as this technique was not available at the time of CMR examination. Finally, we did not investigate the prognostic value of RA strain and SR in DCM patients, which needs further exploration in future research. Nevertheless, the findings herein may offer a tool for assessing such prognostic value.

Conclusions

CMR-FT emerges as a promising approach for the

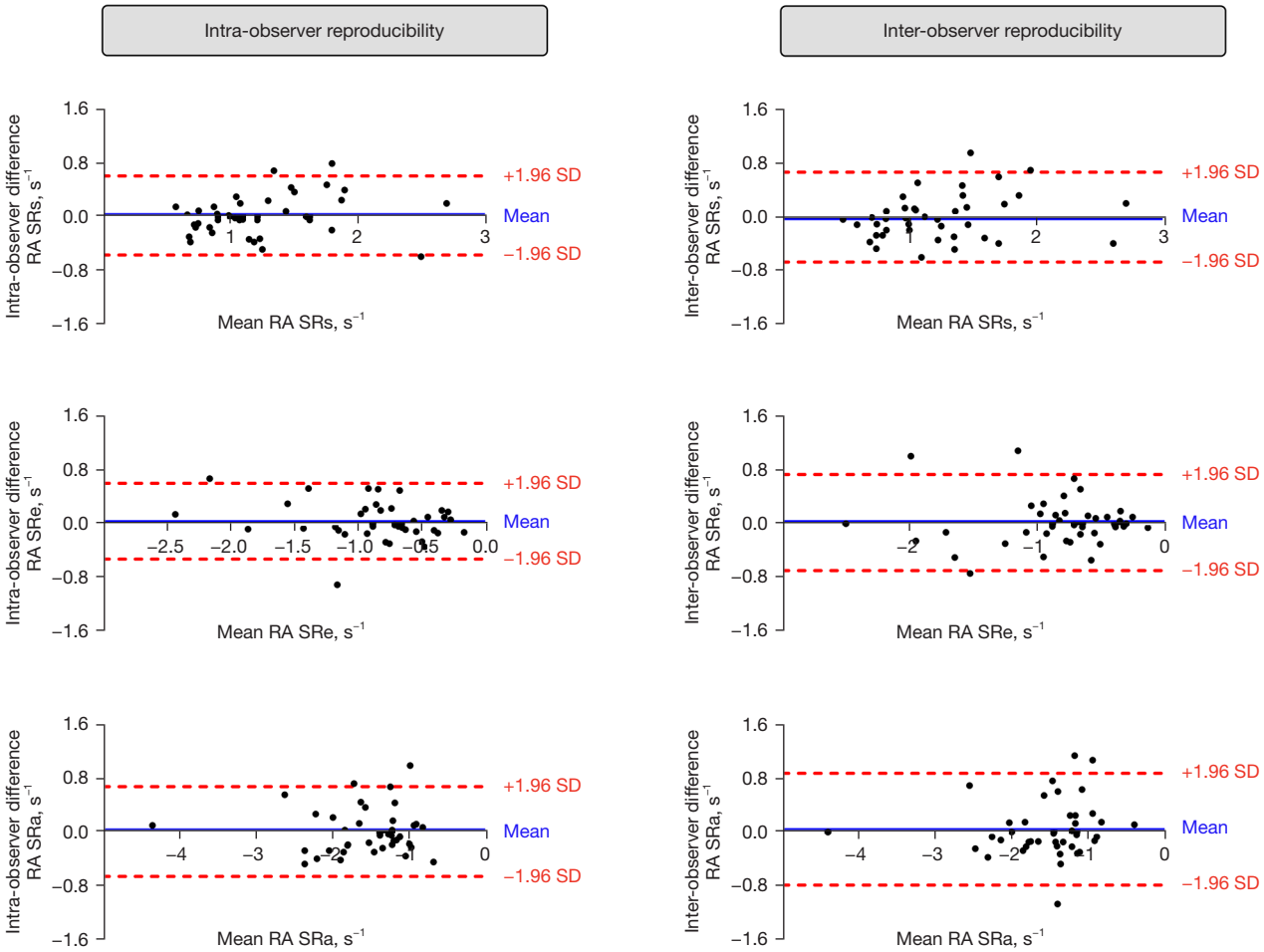

Figure 5 Bland-Altman plots for intra- and inter-observer reproducibility of RA SRs, SRe, and SRa. SD, standard deviation; RA, right atrial; SRs, peak positive SR; SRe, peak early negative SR; SRa, peak late negative SR; SR, strain rate.

quantitative assessment of RA myocardial deformation in patients with DCM. Compared with healthy controls, DCM patients exhibit impaired RA reservoir, conduit, and booster pump function prior to visible RA enlargement. The findings of this study highlight the potential clinical utility of CMR-FT in evaluating RA function and its role in the early detection and management of DCM. However, further research with larger, more diverse cohorts and long-term follow-up is needed to validate the clinical significance of CMR-FT-derived RA deformation parameters in assisting clinical decision-making and improving patient outcomes.

Acknowledgments

We acknowledge Michael C. Lin for language editing in the preparation of this manuscript. Preliminary results of this work were presented at the Cardiothoracic Imaging Annual Meeting of the Chinese Society of Radiology in 2023 (Abstract #PO-020).

Funding: This study was supported by the National Natural Science Foundation of China (No. 81971600), "Pioneer" and "Leading Goose" R&D Program of Zhejiang (No. 2022C03046), and Zhejiang Chinese Medical University Postgraduate Scientific Research Fund Project (No. 2023YKJ08).

Footnote

Reporting Checklist: The authors have completed the STROBE reporting checklist. Available at https://qims.amegroups.com/article/view/10.21037/qims-23-1119/rc

Conflicts of Interest: All authors have completed the ICMJE uniform disclosure form (available at https://qims.amegroups.com/article/view/10.21037/qims-23-1119/coif). The authors have no conflicts of interest to declare.

Ethical Statement: The authors are accountable for all aspects of the work in ensuring that questions related to the accuracy or integrity of any part of the work are appropriately investigated and resolved. The study was conducted in accordance with the Declaration of Helsinki (as revised in 2013). The study was approved by the Ethics Committees of The First Affiliated Hospital of Zhejiang Chinese Medical University (2022-KLS-207-01) and Shenzhen Clinical Medical College of Guangzhou University of Chinese Medicine (2021ECPJ006), and the requirement for individual consent for this retrospective analysis was waived.

References

1. Schultheiss HP, Fairweather D, Caforio ALP, Escher F, Hershberger RE, Lipshultz SE, Liu PP, Matsumori A, Mazzanti A, McMurray J, Priori SG. Dilated cardiomyopathy. Nat Rev Dis Primers 2019;5:32.
2. Finocchiaro G, Merlo M, Sheikh N, De Angelis G, Papadakis M, Olivotto I, Rapezzi C, Carr-White G, Sharma S, Mestroni L, Sinagra G. The electrocardiogram in the diagnosis and management of patients with dilated cardiomyopathy. Eur J Heart Fail 2020;22:1097-107.
3. Weintraub RG, Semsarian C, Macdonald P. Dilated cardiomyopathy. Lancet 2017;390:400-14.
4. Díez-López C, Salazar-Mendiguchía J, García-Romero E, Fuentes L, Lupón J, Bayés-Genis A, Manito N, de Antonio M, Moliner P, Zamora E, Catalá-Ruiz P, Caínzos-Achirica M, Comín-Colet J, González-Costello J. Clinical Determinants and Prognosis of Left Ventricular Reverse Remodelling in Non-Ischemic Dilated Cardiomyopathy. J Cardiovasc Dev Dis 2022;9:20.
5. Ochs A, Riffel J, Ochs MM, Arenja N, Fritz T, Galuschky C, Schuster A, Bruder O, Mahrholdt H, Giannitsis E, Frey N, Katus HA, Buss SJ, André F. Myocardial mechanics in dilated cardiomyopathy: prognostic value of left ventricular torsion and strain. J Cardiovasc Magn Reson 2021;23:136.
6. Nuzzi V, Raafs A, Manca P, Henkens MTHM, Gregorio C, Boscutti A, Verdonschot J, Hazebroek M, Knackstedt C, Merlo M, Stolfo D, Sinagra G, Heymans SRB. Left Atrial Reverse Remodeling in Dilated Cardiomyopathy. J Am Soc Echocardiogr 2023;36:154-62.
7. Li Y, Xu Y, Tang S, Jiang X, Li W, Guo J, Yang F, Xu Z, Sun J, Han Y, Zhu Y, Chen Y. Left Atrial Function Predicts Outcome in Dilated Cardiomyopathy: Fast Long-Axis Strain Analysis Derived from MRI. Radiology 2022;302:72-81.
8. Liu T, Gao Y, Wang H, Zhou Z, Wang R, Chang SS, Liu Y, Sun Y, Rui H, Yang G, Firmin D, Dong J, Xu L. Association between right ventricular strain and outcomes in patients with dilated cardiomyopathy. Heart 2021;107:1233-9.
9. Rai AB, Lima E, Munir F, Faisal Khan A, Waqas A, Bughio S, ul Haq E, Attique HB, Rahman ZU. Speckle Tracking Echocardiography of the Right Atrium: The Neglected Chamber. Clin Cardiol 2015;38:692-7.
10. Kumar S, Vadlamudi K, Kaddoura T, Bobhate P, Goot BH, Elgendi M, Jain S, Colen T, Khoo NS, Adatia I. Active right atrial emptying fraction predicts reduced survival and increased adverse events in childhood pulmonary arterial hypertension. Int J Cardiol 2018;271:306-11.
11. Jain S, Kuriakose D, Edelstein I, Ansari B, Oldland G, Gaddam S, Javaid K, Manaktala P, Lee J, Miller R, Akers SR, Chirinos JA. Right Atrial Phasic Function in Heart Failure With Preserved and Reduced Ejection Fraction. JACC Cardiovasc Imaging 2019;12:1460-70.
12. Hasselberg NE, Kagiyama N, Soyama Y, Sugahara M, Goda A, Ryo-Koriyama K, Batel O, Chakinala M, Simon MA, Gorcsan J 3rd. The Prognostic Value of Right Atrial Strain Imaging in Patients with Precapillary Pulmonary Hypertension. J Am Soc Echocardiogr 2021;34:851-861.e1.
13. Singulane CC, Slivnick JA, Addetia K, Asch FM, Sarswat N, Soulat-Dufour L, Mor-Avi V, Lang RM. Prevalence of Right Atrial Impairment and Association with Outcomes in Cardiac Amyloidosis. J Am Soc Echocardiogr 2022;35:829-835.e1.
14. Miah N, Faxén UL, Lund LH, Venkateshvaran A. Diagnostic utility of right atrial reservoir strain to identify elevated right atrial pressure in heart failure. Int J Cardiol

2021;324:227-32.
15. Liu B, Dardeer AM, Moody WE, Edwards NC, Hudsmith LE, Steeds RP. Normal values for myocardial deformation within the right heart measured by feature-tracking cardiovascular magnetic resonance imaging. Int J Cardiol 2018;252:220-3.
16. Chen Z, Zhang S, Fang A, Shao J, Shen H, Sun B, Guo G, Liu L. Early changes in left ventricular myocardial function by 2D speckle tracking layer-specific technique in neonates with hyperbilirubinemia. Quant Imaging Med Surg 2022;12:796-809.
17. Truong VT, Palmer C, Young M, Wolking S, Ngo TNM, Sheets B, Hausfeld C, Ornella A, Taylor MD, Zareba KM, Raman SV, Mazur W. Right Atrial Deformation Using Cardiovascular Magnetic Resonance Myocardial Feature Tracking Compared with Two-Dimensional Speckle Tracking Echocardiography in Healthy Volunteers. Sci Rep 2020;10:5237.
18. Li Y, Guo J, Li W, Xu Y, Wan K, Xu Z, Zhu Y, Han Y, Sun J, Chen Y. Prognostic value of right atrial strain derived from cardiovascular magnetic resonance in non-ischemic dilated cardiomyopathy. J Cardiovasc Magn Reson 2022;24:54.
19. Gao Y, Pu C, Li Q, Guo Y, Shi J, Zhang Z, Xiang P, Hu X, Wu Y, Zeng Q, Yu R, Hu H, Xu M. Assessment of Right Atrial Function Measured with Cardiac MRI Feature Tracking for Predicting Outcomes in Patients with Dilated Cardiomyopathy. Radiology 2024;310:e232388.
20. Raafs AG, Vos JL, Henkens MTHM, Slurink BO, Verdonschot JAJ, Bossers D, Roes K, Gerretsen S, Knackstedt C, Hazebroek MR, Nijveldt R, Heymans SRB. Left Atrial Strain Has Superior Prognostic Value to Ventricular Function and Delayed-Enhancement in Dilated Cardiomyopathy. JACC Cardiovasc Imaging 2022;15:1015-26.
21. Gao Y, Zhang Z, Zhou S, Li G, Lou M, Zhao Z, Zhao J, Li K, Pohost GM. Reference values of left and right atrial volumes and phasic function based on a large sample of healthy Chinese adults: A cardiovascular magnetic resonance study. Int J Cardiol 2022;352:180-7.
22. Krittanawong C, Maitra NS, Hassan Virk HU, Farrell A, Hamzeh I, Arya B, Pressman GS, Wang Z, Marwick TH. Normal Ranges of Right Atrial Strain: A Systematic Review and Meta-Analysis. JACC Cardiovasc Imaging 2023;16:282-94.
23. Kowallick JT, Morton G, Lamata P, Jogiya R, Kutty S, Hasenfuß G, Lotz J, Nagel E, Chiribiri A, Schuster A. Quantification of atrial dynamics using cardiovascular magnetic resonance: inter-study reproducibility. J Cardiovasc Magn Reson 2015;17:36.
24. Tigen K, Karaahmet T, Dundar C, Cincin A, Ozben B, Guler A, Gurel E, Sunbul M, Basaran Y. Right ventricular and atrial functions in patients with nonischemic dilated cardiomyopathy. Wien Klin Wochenschr 2015;127:877-83.
25. Pinsky MR. Cardiopulmonary Interactions: Physiologic Basis and Clinical Applications. Ann Am Thorac Soc 2018;15:S45-8.
26. Borlaug BA, Obokata M. The Other Atrium in Heart Failure. JACC Cardiovasc Imaging 2019;12:1471-3.
27. Vollmar AC, Aupperle H. Cardiac pathology in Irish wolfhounds with heart disease. J Vet Cardiol 2016;18:57-70.
28. De Bonis M, Lapenna E, Sorrentino F, La Canna G, Grimaldi A, Maisano F, Torracca L, Alfieri O. Evolution of tricuspid regurgitation after mitral valve repair for functional mitral regurgitation in dilated cardiomyopathy. Eur J Cardiothorac Surg 2008;33:600-6.
29. Bogaert J, Symons R, Rafouli-Stergiou P, Droogné W, Dresselaers T, Masci PG. Assessment of Right-Sided Heart Failure in Patients with Dilated Cardiomyopathy using Magnetic Resonance Relaxometry of the Liver. Am J Cardiol 2021;149:103-11.
30. Järvinen VM, Kupari MM, Poutanen VP, Hekali PE. Right and left atrial phasic volumetric function in mildly symptomatic dilated and hypertrophic cardiomyopathy: cine MR imaging assessment. Radiology 1996;198:487-95.
31. Cao Z, Jia Y, Zhu B. BNP and NT-proBNP as Diagnostic Biomarkers for Cardiac Dysfunction in Both Clinical and Forensic Medicine. Int J Mol Sci 2019;20:1820.
32. Shen S, Ye J, Wu X, Li X. Association of N-terminal pro-brain natriuretic peptide level with adverse outcomes in patients with acute myocardial infarction: A meta-analysis. Heart Lung 2021;50:863-9.
33. Wu G, Liu J, Wang S, Yu S, Zhang C, Wang D, Zhang M, Yang Y, Kang L, Zhao S, Hui R, Zou Y, Wang J, Song L. N-terminal pro-brain natriuretic peptide and sudden cardiac death in hypertrophic cardiomyopathy. Heart 2021;107:1576-83.
34. Qu YY, Buckert D, Ma GS, Rasche V. Quantitative Assessment of Left and Right Atrial Strains Using Cardiovascular Magnetic Resonance Based Tissue Tracking. Front Cardiovasc Med 2021;8:690240.
35. Leng S, Dong Y, Wu Y, Zhao X, Ruan W, Zhang G, Allen JC, Koh AS, Tan RS, Yip JW, Tan JL, Chen Y, Zhong L. Impaired Cardiovascular Magnetic Resonance-Derived Rapid Semiautomated Right Atrial Longitudinal Strain

Is Associated With Decompensated Hemodynamics in Pulmonary Arterial Hypertension. Circ Cardiovasc Imaging 2019;12:e008582.
36. Tello K, Dalmer A, Vanderpool R, Ghofrani HA, Naeije R, Roller F, Seeger W, Wiegand M, Gall H, Richter MJ. Right ventricular function correlates of right atrial strain in pulmonary hypertension: a combined cardiac magnetic resonance and conductance catheter study. Am J Physiol Heart Circ Physiol 2020;318:H156-64.
37. Kagami K, Harada T, Yoshida K, Amanai S, Kato T, Wada N, Adachi T, Obokata M. Impaired Right Atrial Reserve Function in Heart Failure with Preserved Ejection Fraction. J Am Soc Echocardiogr 2022;35:836-45.
38. Schuster A, Backhaus SJ, Stiermaier T, Navarra JL, Uhlig J, Rommel KP, Koschalka A, Kowallick JT, Bigalke B, Kutty S, Gutberlet M, Hasenfuß G, Thiele H, Eitel I. Impact of Right Atrial Physiology on Heart Failure and Adverse Events after Myocardial Infarction. J Clin Med 2020;9:210.
39. Dziewięcka E, Wiśniowska-Śmiałek S, Karabinowska A, Holcman K, Gliniak M, Winiarczyk M, Karapetyan A, Kaciczak M, Podolec P, Kostkiewicz M, Hlawaty M, Leśniak-Sobelga A, Rubiś P. Relationships between Pulmonary Hypertension Risk, Clinical Profiles, and Outcomes in Dilated Cardiomyopathy. J Clin Med 2020;9:1660.

Cite this article as: Gao Y, Shi J, Shi Y, Guo L, Zhou S, Zhang F, Guo Y, Gao C, Kong N, Xiang P, Lou M, Xu M. Feasibility and reproducibility of cardiovascular magnetic resonance-feature tracking for quantitative right atrial function in dilated cardiomyopathy patients. Quant Imaging Med Surg 2024;14(5):3312-3325. doi: 10.21037/qims-23-1119

